Divergent resistance at the Dirac point in graphene: Evidence for a transition in a high magnetic field

Joseph G. Checkelsky, Lu Li,* and N. P. Ong
Department of Physics, Princeton University, Princeton, New Jersey 08544, USA
(Received 4 February 2009; published 24 March 2009)

We have investigated the behavior of the resistance of graphene at the $n=0$ Landau level in an intense magnetic field H. Employing a low-dissipation technique (with power $P<3$ fW), we find that at low temperature T, the resistance at the Dirac point $R_0(H)$ undergoes a 1000-fold increase from ~ 10 kΩ to 40 MΩ within a narrow interval of field. The abruptness of the increase suggests that a transition to an insulating ordered state occurs at the critical field H_c. Results from five samples show that H_c depends systematically on the disorder, as measured by the offset gate voltage V_0. Samples with small V_0 display a smaller critical field H_c. Empirically, the steep increase in R_0 fits accurately a Kosterlitz-Thouless-type correlation length over three decades. The curves of R_0 vs T at fixed H approach the thermal-activation form with a gap $\Delta \sim 15$ K as $H \rightarrow H_c^-$, consistent with a field-induced insulating state.

DOI: 10.1103/PhysRevB.79.115434 PACS number(s): 73.63.−b, 73.21.−b, 73.43.−f

I. INTRODUCTION

In graphene, the low-energy states display a linear energy-momentum dispersion described by the Dirac Hamiltonian. The observation of the integer quantum Hall (QH) effect by Novoselov *et al.*[1–3] and Zhang and co-workers[4–6] has sparked intense interest in this novel two-dimensional (2D) system. In a strong magnetic field H, the states are quantized into Landau levels (LLs). As a result of the Dirac dispersion, the energy E_n of the LL (of index n) increases with the flux density B as $\sqrt{B}$, viz., $E_n=\mathrm{sgn}(n)\sqrt{2e\hbar v_F^2 B|n|}$, where v_F is the Fermi velocity, e is the electron charge, and h is Planck's constant. The Hall conductivity is observed to be accurately quantized as $\sigma_{xy}=(4e^2/h)[n+\frac{1}{2}]=\nu e^2/h$, where e is the electron charge, $2\pi\hbar$ is Planck's constant, and ν is the sublevel index. A key question is the nature of the ground state at the Dirac point. In intense H, theory predicts interesting broken-symmetry states driven by exchange and interaction. These are characterized as quantum Hall ferromagnetism (QHF) (Refs. 7–12) or excitonic condensation.[13–16] These collective states imply the existence of field-induced phase transitions but the experimental situation is rather unsettled. Moreover, the proposed[12,17,18] existence of counterpropagating edge (CPE) modes at the Dirac point has further enriched the theoretical debate. Is the high-field Dirac point a QH insulator or a QH metal?

Recently, we reported[19] that the resistance at the Dirac point R_0 begins to increase steeply at $B=10-12$ T, suggesting a transition to an insulating state. However, the results left open several key questions. Because R_0 increased by only 1 decade (to 0.2 MΩ),[19] we could not establish that the high-field state is truly insulating. In graphene, the extreme sensitivity to thermal runaway has been highly problematical for researching its high-H ground state.[5,6,19] Adopting a low-dissipation technique to avoid self-heating, we have measured the divergence in R_0 to 40 MΩ($\sim 1500h/e^2$) in three samples. Remarkably, the divergence is accurately described over three decades by the Kosterlitz-Thouless (KT) correlation length. The *singular* nature of the divergence provides strong evidence that a 2D transition to an insulating state occurs when B exceeds a critical field H_c. The systematic variation in H_c with $|V_0|$ (the gate voltage needed to bring the chemical potential μ to the Dirac point) implies that disorder is very effective in delaying H_c to higher-field values. In all samples investigated to date, the transition to the insulating state is reached in fields below 35 T.

II. EXPERIMENTAL DETAILS

Empirically, problems associated with self-heating in graphene become serious when the power dissipated P exceeds ~ 10 pW for bath temperature $T_b<1$ K. As discussed in the Appendix, self-heating below 1 K leads to a number of spurious features caused by thermal instability in the sample. We adopted a simple voltage-controlled technique with ultralow dissipation that avoids this difficulty and allows the divergence in R_0 to be measured reliably to 40 MΩ. An ac source maintains a fixed voltage amplitude (40 μV) across the sample in series with a 100 kΩ resistor (details are given in the Appendix). By phase-sensitive detection of both the current I and the voltage V_{xx}, we have made four-probe measurements of R_0 with ultralow dissipation (P decreases from ~ 3 fW at 10 T to 40 aW above 25 T). Moreover, for $T<1.5$ K, the sample is immersed in liquid ^{3}He so that the electrons in graphene are in direct contact with the bath. The largest reliably measured R_0 is now 40 MΩ (limited by the input impedance 100 MΩ of the preamplifier). The present results provide an enlarged view of the interesting region in which R_0 diverges. The samples K52 and J24 have offset voltages V_0 much larger than that in K7, the sample investigated in detail in Ref. 19. All samples except J18 were measured as fabricated. Sample J18 was subject to a $\frac{1}{2}$ hr anneal in He gas at 80 C which decreased V_0 to 8 V. However its large H_c suggests that its initial value of V_0 (before annealing) is very large. In samples K52, J18, and J24, the spacings a between voltage leads are 3.5, 2.75, and 3 μm, while the widths w are 3, 3, and 2 μm, respectively.

III. FIELD DEPENDENCE OF R_0

Figure 1 (main panel) shows the curves of R_0 vs H in K52 at temperatures $T=0.3-27$ K. As evident in the curves at 0.3

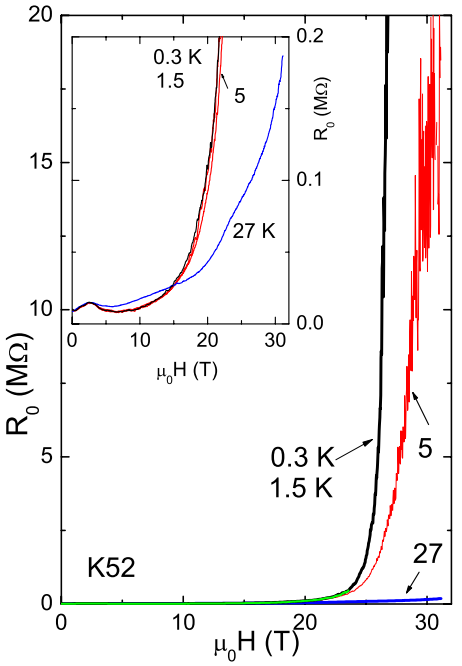

FIG. 1. (Color online) Main panel: divergence of the resistance R_0 at the Dirac point with B at $T=0.3$, 1.5, 5, and 27 K (sample K52). At 27 K, the increase in R_0 is quite moderate (to 190 kΩ at $H=31$ T). At $T=0.3$ K, however, R_0 exceeds 20 MΩ above 27 T. The curves at 0.3 and 1.5 K undergo a 1000-fold increase (40 kΩ to 40 MΩ) in the narrow field interval 17–27 T. In high B, the 5 K curve deviates significantly from them. The inset shows the behavior of R_0 vs H in greatly expanded scale (×100). The voltage-regulated technique used for these measurements dissipates ~3 fW at 10 T and 40 aW above 25 T.

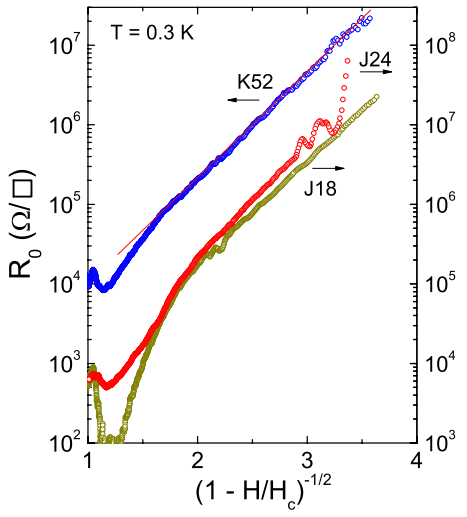

FIG. 2. (Color online) Plot of R_0 vs $1/\sqrt{1-h}$ for samples K52, J18, and J24 at $T=0.3$ K, where $h=H/H_c$ (the curve for K52 is displaced by 1 decade for clarity). R_0 is expressed as sheet resistance (Ω/□). For each sample, H_c is the optimal value that gives the best straight-line fit vs $1/\sqrt{1-h}$ (curvature is noticeable if H_c is altered by ±0.1 T from this value). For samples K52, J18, and J24, H_c equals 29.1, 32.1, and 35.5 T, respectively. For K52, the thin solid line is the expression $R_\xi(h)=440\exp[2b/\sqrt{1-h}]$, with $b=1.54$. The data match $R_\xi(h)$ very well over nearly three decades in R_0.

and 1.5 K, R_0 undergoes a very steep divergent increase when H exceeds ~25 T. The region just before the divergence occurs is shown in greatly expanded scale in the inset. At 27 K, the increase in R_0 is relatively modest (~20) between $B=0$ and 31 T (inset). However, as T decreases to 5 K, the increase steepens sharply, as reported[19] for K7. Further cooling from 5 to 0.3 K changes the profile only very slightly. In the main panel, the curves at 0.3 and 1.5 K (which cannot be distinguished) show that R_0 diverges to 40 MΩ, with a slope that steepens rapidly with H. The three decade increase (40 kΩ→40 MΩ) occurs within the narrow interval 17–27 T. We find that the observed divergence is too steep to fit a power law of the kind $R_0 \sim (H_c - H)^{-\alpha}$, with $\alpha > 0$ and H_c as a critical field.

As in Ref. 19, we compare the divergence with that predicted for the KT transition. In 2D systems described by the XY model, the ordered phase is destroyed at the KT transition by unbinding of pairs of topological excitations (e.g., vortices). As the transition here is induced by varying the applied field H, we replace the reduced temperature t by the reduced field $h=H/H_c$, with H_c as the critical field. In the limit $h \to 1^-$, the KT correlation length ξ diverges as

$$\xi = a \exp[b/\sqrt{1-h}], \tag{1}$$

where a is the lattice parameter and b is a number ~1.

The quality of the fit to Eq. (1) is best revealed in a plot of log R_0 vs the quantity $1/\sqrt{1-h}$. In Fig. 2, we have plotted log R_0 in three samples K52, J19, and J24 against $1/\sqrt{1-h}$. In each sample, the value of H_c is adjusted to maximize the high-field portion of the plot that falls on a straight line (this is the only adjustment made). In samples K52, J18, and J24, the inferred values of H_c are 29.1, 32.1, and 35.5 T, respectively. The values of R_0 in K52 fit the straight line representing the expression $R_\xi(h)=440\exp[2b/\sqrt{1-h}]$, with $H_c=29.1$ T and $b=1.54$. The value of b is consistent with the KT transition. The 3 decade span is a strong evidence that Eq. (1) accurately describes the divergence in R_0 and supports the inference that at low T, we are observing a 2D KT-type phase transition to a high-field ordered state that is insulating.

The significant spread of H_c inferred from the fits in Fig. 2 is in accord with Ref. 19 which reported that H_c correlates with the offset voltage V_0. In Fig. 2, the samples K52, J18, and J24 display a much larger critical field H_c than the sample K7 (with $V_0=1$ V and $H_c=18$ T) studied in detail in Ref. 19. Figure 3 plots together, in log-log scale, the curves of R_0 vs H in the five samples for which we have detailed high-field transport results. The systematic shift to higher fields of the divergence (in the order K22, K7, K52, and J24) is matched by the increase in their V_0 (−0.5, 1, 3, 20, and 24 V, respectively). The value of V_0 before annealing in J18 is not known. The dependence of H_c on V_0 is nonlinear. Initially (for $0 < V_0 < 4$V), H_c increases rapidly but appears to increase rather slowly when V_0 exceeds 20 V.

From a study of how V_0 affects the zero-field transport, we have obtained evidence that the zero-field mobility μ_e is

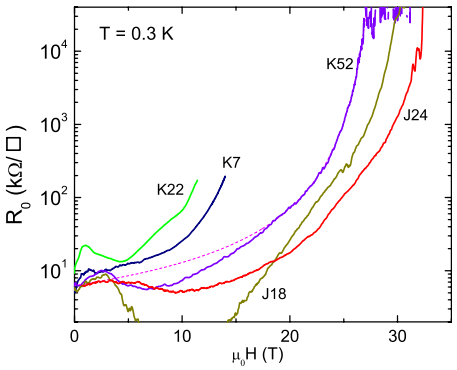

FIG. 3. (Color online) Comparison of the curves of R_0 vs H at 0.3 K in log-log scale in five samples K7, K22, K52, J18, and J24 with gate-voltage offsets $V_0=1$, −0.6, 3, 20, and 24 V, respectively (V_0 before annealing is not known in J18). R_0 is expressed as sheet resistance $\Omega/\square$. In K7 and K22 (which have small $|V_0|$), the divergence in R_0 occurs at a lower H (Ref. 19). The femtowatt-dissipation technique applied to K52, J18, and J24 was not available for K7 and K22 (their curves were limited to $R_0<0.3$ MΩ). The dashed curve is the fit of the K52 data to R_ξ.

strongly suppressed if V_0 is large. In Fig. 4, we display curves of R_{xx} vs the unshifted gate voltage V_g in a batch of samples that includes K22. The curves are taken at 295 or 4 K (as indicated). In each sample, the width ΔV_g of the peak at the Dirac point directly measures $1/\mu_e$. Clearly, the width increases dramatically with V_0. These results support the inference that a large offset V_0 gives rise to large electronic disorder which enhances disorder scattering and suppresses μ_e. In turn, in an intense field, the transition field H_c is pushed to higher values. While these correlations do not exclude other factors that may influence H_c, we have found that V_0 is the single most reliable predictor of the field scale at which the divergence onsets at low T.

IV. DOPING DEPENDENCE

Further insight into the nature of the divergence is obtained by viewing the behavior of the longitudinal resistance

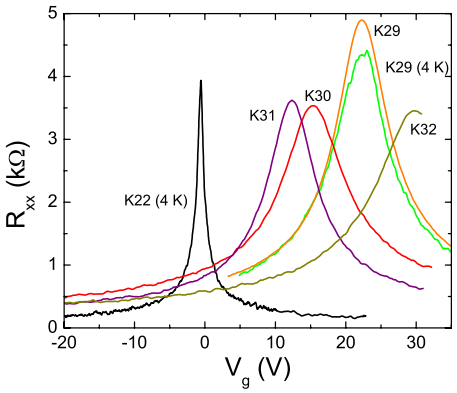

FIG. 4. (Color online) Curves of the longitudinal resistance R_{xx} vs unshifted gate voltage V_g in zero H in a series of samples at 295 and 4 K (as indicated). The width of the peak in R_{xx} increases systematically with V_0 (located by the peak position). This implies that the mobility μ_e is very low in samples with large V_0.

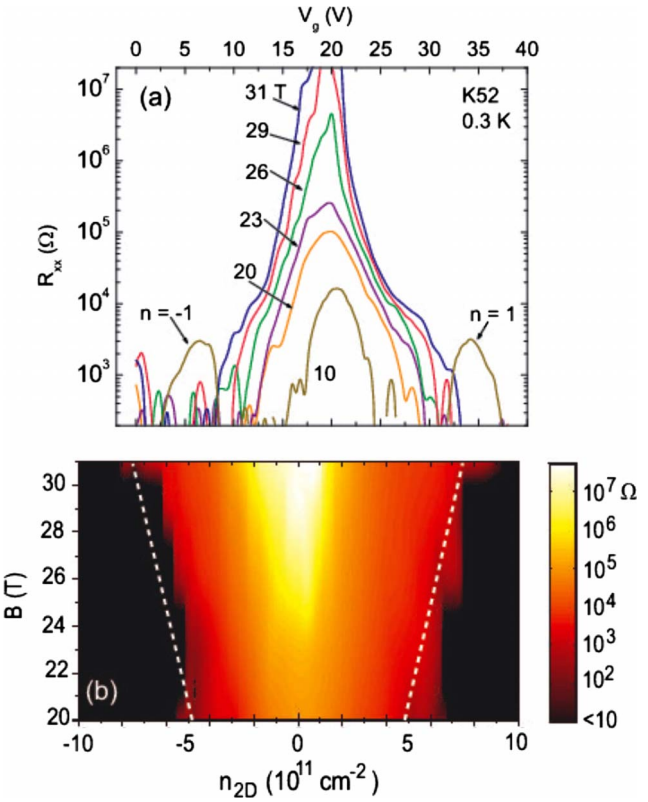

FIG. 5. (Color online) Variation in R_{xx} (sample K52) vs the gate voltage V_g in the interval ($0<V_g<38$ V), with B fixed at selected values 10–31 T, and $T=0.3$ K (panel a). At $B=10$ T, the central peak ($n=0$ LL) is well separated from the LL peaks labeled as $n=\pm 1$. At $B=20$ T and higher, the $n=\pm 1$ LLs fall outside the gate window. With increasing B, the central peak increases rapidly and broadens. At the maximum B (31 T), R_{xx} at the Dirac point ($V_g=20$ V) diverges to values above 40 MΩ. The voltage-regulated technique has poor resolution when R_{xx} falls below 0.3 kΩ. Panel (b) shows the contour plot of $R_{xx}(n_{2D},B)$ at 0.3 K in the n_{2D}-B plane (color bar of R_{xx} shown on right). The dashed lines trace the sublevel degeneracy $1/2\pi\ell_B^2$. The density is given by $n_{2D}=CV_g/Ae$ where C and A are the capacitance and area of the device, respectively ($C/A=1.14\times10^{-4}$ Fm^{-2}).

R_{xx} vs V_g in a narrow gate window around the Dirac point at fixed B (with T kept at 0.3 K). Figure 5(a) displays a series of curves of R_{xx} (in log scale) vs V_g in K52 for fields $10\le H\le 31$ T. At 10 T, R_{xx} displays three well-separated peaks corresponding to $n=0$ LL at 20 V and the $n=\pm 1$ LLs at 6 and 38 V, respectively. For $H\ge 20$ T, the $n=\pm 1$ levels move out of the gate-voltage window. We focus on the divergent enhancement of the central peak as B increases to 31 T. The key feature is that R_{xx} at the Dirac point ($V_g=20$ V) rises most rapidly especially for $B>25$ T.

It is instructive to view R_{xx} (at 0.3 K) as a contour plot in the n_{2D}-B plane where n_{2D} is the 2D density of carriers doped by gating [Fig. 5(b)]. The color bar (right) gives the magnitude of R_{xx}. Interestingly, the steep increase in R_{xx} with B is confined to the region between the dashed lines, which trace the sublevel degeneracy $1/2\pi\ell_B^2$. This suggests that only the states within the lowest sublevels (on either side of $\nu=0$) are affected by the opening of the gap Δ. The contours

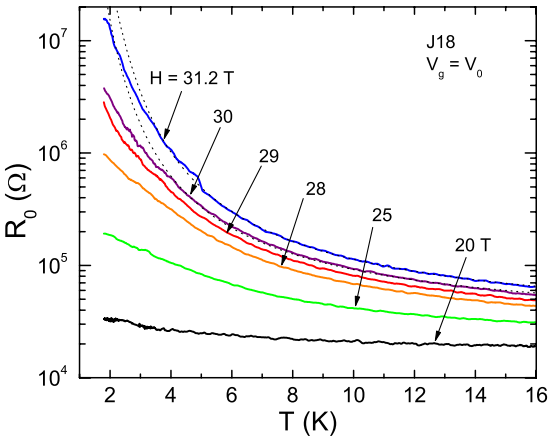

FIG. 6. (Color online) The T dependence of R_0 in sample J18 with H fixed at selected values in the interval $20<H<31.2$ T. As H approaches H_c (32.1 T), R_0 approaches the thermally activated form $e^{\Delta/T}$. The thin dashed curves are fits to this form with the gap $\Delta=12.9$ and 14.7 K at $H=30$ and 31.2 T, respectively. At the highest field (31.2 T), R_0 increases by a factor of 310 between 16 and 2 K.

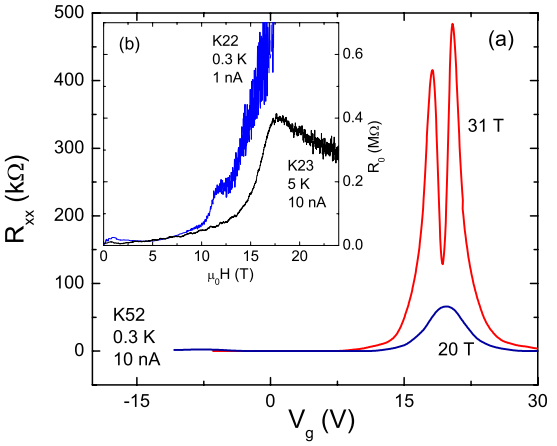

FIG. 7. (Color online) Spurious features caused by sample self-heating in graphene. Panel (a) shows a gate-sweep measurement at $T=0.3$ K of R_{xx} vs V_g in K52, with I fixed at 10 nA (dc). At $B=31$ T (red curve), severe self-heating inverts the peak at the Dirac point (as shown in Fig. 1, R_0 actually exceeds 40 MΩ). Heating effects are less severe in the 20 T curve. Panel (b) displays curves of R_0 vs B measured in samples K22 (at 0.3 K) and K23 (at 5 K) with I fixed at 1 and 10 nA (dc), respectively. When $R_0>0.2$ MΩ, self-heating produces the spurious shoulders and broad peaks, whose positions and shapes depend on I.

appear to converge to a rounded cusp at $n_{2D}=0$ but with a curvature that increases rapidly with B. At the largest R_{xx} (white region), the contour resembles a narrow sharp wedge. The contour pattern suggests that H_c increases very rapidly from the value 29.1 T, as $|n_{2D}|$ deviates from 0.

The physical picture implied by the results is that at the Dirac point, a field-induced transition to a gapped insulating state occurs at H_c. The value of H_c is highly sensitive to slight deviations away from the exact charge neutrality (Fig. 5). As we decrease H below H_c, the ordered state is unstable to the spontaneous unbinding of (vortexlike) topological excitations which have a mean spacing of ξ [Eq. (1)]. Because R_0 fits accurately to ξ^2 over three decades, we infer that the conductance scales as the density of excitations. Hence the excitations are charged, and they carry the entire current I in the limit $T\rightarrow 0$. As this conduction channel is qualitatively distinct from thermally activated carriers, it may account for the unusual "saturation" behavior of R_0 vs T.[19] As $T\rightarrow 0$, with H fixed near H_c, the conduction crosses over at 1 K from a steep thermally activated channel to a T-independent channel carried by the excitations [Fig. 1(b)].

V. TEMPERATURE DEPENDENCE

The T dependence of R_0 in J18 with H fixed at selected values is displayed in a semilog scale in Fig. 6. At the relatively high field $H=20$ T, the twofold increase in R_0 between 16 and 2 K is quite modest. However, above 20 T, the T dependence steepens rapidly. As H is increased toward the critical H_c(=32.1 T), the profile of R_0 moves ever closer to the activated form $R_0\sim e^{\Delta/T}$. We have plotted fits to the activated form (dashed curves) at the two highest fields $H=30$ and 31.2 T. At the highest H, the measured R_0 tracks closely the dashed curve until T falls below 3 K where it deviates downward. As H decreases further from H_c, the deviations start at a higher T. The gap value Δ equals 12.9 and 14.7 K at 30 and 31.2 T, respectively. The latter provides an estimate of the energy gap in the ordered state for J18. Establishing that R_0 is thermally activated when $H>H_c$ is an essential goal, as it shows that the ground state above H_c is a true insulator with a well-defined gap order parameter (as opposed to a state in which the carriers are strongly localized). Although the curves in Fig. 6 come close to establishing this result, measurements of R_0 vs T in samples with more accessible H_c are desirable.

Interestingly, throughout the pretransition region ($20<H<H_c$), R_0 also displays large increases with decreasing T. The carriers are strongly affected by the impending insulating state. We interpret these changes as reflecting very strong fluctuations in the order parameter that characterizes the ordered insulating phase. The strong T dependence is also apparent in the fixed-T curves shown in Fig. 1.

Quite apart from the thermal-activation argument, there are other evidences to suggest that the divergence is not consistent with electron localization. As evident from measuring the widths of the peaks of R_{xx} vs V_g taken in zero B, samples with smallest $|V_0|$ are the least disordered. The electron mobility μ_e decreases from ~2.5 to 0.5 T^{-1} as $|V_0|$ increases from 0.5 to 20 V. With this trend in mind, we compare in Fig. 3 the profiles of R_0 vs B in K52 with K7 and K22.[19] In samples K22 and K7 (with $V_0=-0.6$ and 1 V, respectively), the divergence in R_0 is apparent in relatively low B (below 12 T). By contrast, we must go to much higher fields (>20 T) in K52. The dashed line is the fit to R_ξ in K52 ($H>18$ T) described above.

In the localization scenario, the observed divergence of R_0 in strong field is explained by postulating that B induces localization of the electrons. However, applying this reasoning to the three samples in Fig. 2, we would conclude that a modest B is sufficient to trigger the localization in clean

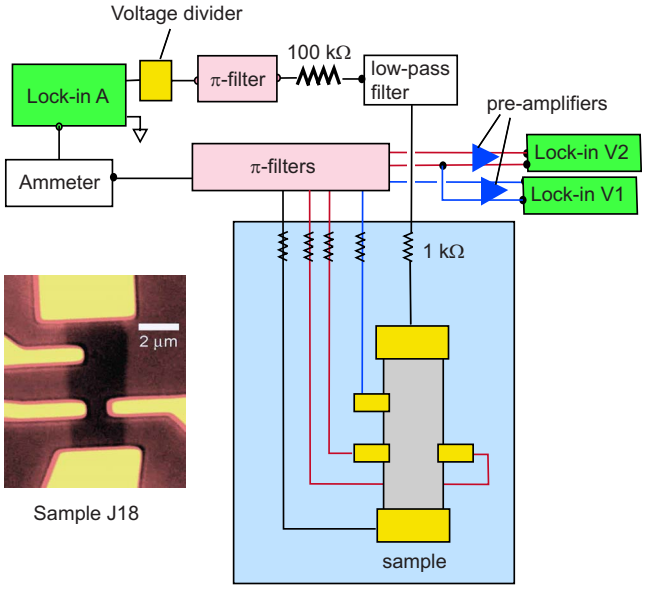

FIG. 8. (Color online) Schematic of the low-dissipation voltage-regulated circuit used in the experiment. Lock-in (amplifier) A produces a regulated voltage emf (3 Hz) that is reduced to an amplitude of 40 μV by a 100:1 voltage divider. The signal goes through a π filter, a buffer resistor (100 kΩ), and a low-pass filter before entering the dewar. The ac current passing through the graphene sample is measured by the picoammeter (Keithley), whose output is phase detected by lock-in A. The longitudinal voltage V_{xx} and Hall voltage V_{xy} are phase detected by lock ins V_1 and V_2, respectively, after transmission through a bank of π filters and high-impedance (100 MΩ) preamplifiers. As shown, all wires entering the dewar are buffered by 1 kΩ nichrome thin-film ceramic resistors. The inset (lower left) shows sample J18.

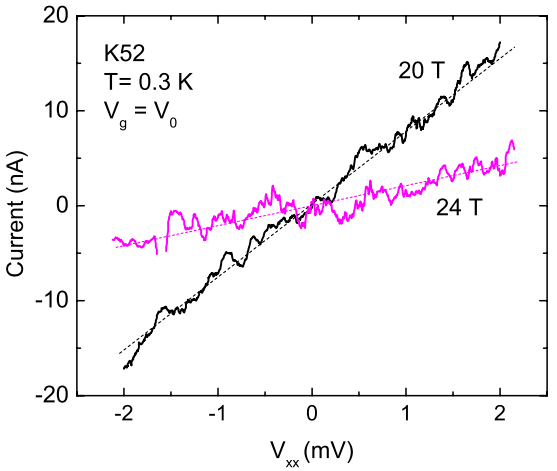

FIG. 9. (Color online) The current-voltage curves measured at the Dirac point ($V_g=V_0$) in sample K52 at $T=0.3$ K at the two fields $H=20$ and 24 T (using the circuit in Fig. 8). The linearity of I vs V_{xx} implies that at these fields, self-heating is not observable at these power-dissipation levels (the dashed lines are guides to the eyes).

samples but very intense fields are needed in dirtier samples. This implies that disorder and field act in opposition to bring about localization, which is in conflict with physical intuition. In addition, localization induced by B cannot lead to the singular divergence observed in R_0 (Fig. 2). For these reasons, we believe that localization is not a viable explanation for the divergence in R_0.

VI. DISCUSSION

In the absence of Zeeman splitting and electron-electron interaction, the $n=0$ LL is fourfold degenerate corresponding to the (physical) spin degeneracy indexed by $\sigma=\pm 1$ and the K and K' valley degeneracy indexed by $\tau=\pm 1$. At $\nu=0$, the energy of the $n=0$ LL, E_s^τ, is zero. The effect of interaction in producing a broken-symmetry ground state has been investigated by several groups. To discuss our experiment, it is convenient to distinguish two different theoretical scenarios for the $n=0$ LL.

In one scenario, the QHF models, the exchange energy $E_{\rm ex}\sim\sqrt{B}$ leads to ferromagnetic polarization of the physical spins.[7,8,10,12,17] This produces a spin gap in the bulk without affecting the valley degeneracy, i.e., $E_\sigma^\tau=\sigma(\mu_B B+E_{\rm ex})$ with μ_B as the Bohr magneton. Near the edge of the sample, the residual valley degeneracy is lifted by the edge potential. An important consequence of the QHF scenario at $\nu=0$ is the existence of spin-filtered CPE modes which result in a residual conductance of $2e^2/h$ regardless of the magnitude of the spin gap in the bulk.[12,17,18] [In principle, the CPE modes are not present if the exchange polarizes instead the valleys to produce the bulk gap (this involves the same exchange energy $E_{\rm ex}$). However, most investigators favor the spin-polarization scenario in graphene because it is augmented by the Zeeman energy $\mu_B B$ (the valley-polarization scenario is also called the QHF following the original usage[20] in quadratic bilayer GaAs-based devices).]

In the second scenario, called magnetic catalysis,[11,13–16] the field component $B_\perp$ normal to the graphene sheet triggers electron-hole condensation. The instability introduces a mass term to the Dirac equation which leads to the order parameter[13–15] $\langle\bar{\Psi}\Psi\rangle=\Sigma_{\tau\sigma}(|\psi_{\tau A\sigma}|^2-|\psi_{\tau B\sigma}|^2)$, where $\psi_{\tau A\sigma}$ and $\psi_{\tau B\sigma}$ are the wave functions of electrons of spin σ and valley τ at sites A and B, respectively. The instability—a solid-state realization of chiral-symmetry breaking in (2+1)D (Ref. 21)—results in preferential occupation of, say, the A sublattice sites over the B sites and drives the system into an insulating state. Significantly, the instability is strongest for $n=0$.

The steep increase in R_0 vs H first reported in Ref. 19 implies that at large H, the ground state at the Dirac point has a resistance at least 20 times larger than the quantum h/e^2. Although the measurements were limited to $R_0<0.3$ MΩ, the upturn appeared to diverge at a critical field H_c, suggestive of a singular field dependence. The findings are clearly at odds with the existence of CPE modes (see, however, the results in Ref. 18).

In the present report, we have extended by a factor of 200 the range of resistance measurements and shown that at 0.3 K, the increase in R_0 is truly divergent as well as singular. Moreover, this behavior has been observed in all samples investigated to date by us in high fields. The evidence

amassed clearly establishes that the high-field ground state at the Dirac point is a true insulator (at least for samples prepared on a SiO_2 substrate). Ipso facto, the CPE modes do not exist in the insulating state. However, our results do not preclude them at low fields.

Lately, several groups have considered how the CPE modes are affected by intense field. A very interesting possibility is that an intense field destroys the CPE modes in a field-induced transition. It has been pointed out to us that the CPE modes are not protected against two-particle exchange scattering with spin flip.[22] As the exchange energy increases with B, the increased scattering rate could lead to a gap in the edge modes.

In the magnetic catalysis scenario, Gorbar[15] recently considered the competition between the mass gap $\langle\bar{\Psi}\Psi\rangle$ and the spin gap (augmented by Zeeman energy) and inferred that CPE states exist only above a critical field B_{cr}.

Shimshoni *et al.*[23] proposed that scattering off magnetic impurities can lead to strong localization of electrons in CPE modes which can mimic a KT transition. However, this scenario needs to be reconciled with the observed nearly activated behavior of R_0 as well as the variation in H_c with V_0 in different samples.

ACKNOWLEDGMENTS

We thank H. A. Fertig, P. A. Lee, D. Abanin, V. A. Miransky, E. Shimshoni, F. D. M. Haldane, and D. N. Sheng for valuable comments, and acknowledge support from NSF-MRSEC under Grant No. DMR-0819860 and from the Princeton Center for Complex Materials. The experiments were performed at the National High Magnetic Field Laboratory, which is supported by NSF under Cooperative Agreement No. DMR-084173, by the State of Florida and by the Department of Energy.

APPENDIX

Near the Dirac point, resistance traces are strongly distorted when the Ohmic heating P exceeds 10 pW at bath temperatures T_b below 1 K. As examples, we plot in Fig. 7 resistance traces (with I fixed). In panel a, the inferred curve of R_{xx} vs V_g, measured with $B=31$ T, $I=10$ nA, and $T=0.3$ K, shows a pronounced dip near the Dirac point caused by self-heating instability (the true R_0 exceeds 10 MΩ). Panel b shows "R_0" vs B measured at fixed I. In the curve for K23 (at 5 K), self-heating reverses the trend of R_0. The downturn is avoided when I is decreased to 1 nA, but the measured curve (in K22 at 0.3 K) is still greatly suppressed from the true divergent profile.

Figure 8 is a schematic of the measuring circuit employed in the ultralow-dissipation technique. A nominally constant ac voltage (~40 μV) of frequency 3 Hz is applied across the sample in series with a 100 kΩ buffer resistor. The current passing through the sample is measured by a Keithley picoammeter whose output is phase detected by the lock-in amplifier A. Simultaneously, the longitudinal voltage V_{xx} and Hall voltage V_{xy} are phase detected by two other lock ins. As shown, all wires entering the dewar are filtered and buffered to exclude extraneous rf signals which may be a potential source of sample heating.

Using the ultralow-dissipation technique, we completely avoid the thermal runaway problems illustrated in Fig. 7. At selected fields, we have performed I-V measurements to check that self-heating is not skewing the results even at our lowest T (0.3 K). Figure 9 shows curves of I vs V_{xx} at the Dirac point in K52 at $T=0.3$ K with H fixed at 20 and 24 T. The linearity implies that self-heating is not observable up to a bias voltage of 2 mV. Since all the curves displayed in the main text were taken with a bias of 40 μV, we are comfortably within the Ohmic regime.

*Present address: Department of Physics, MIT.

[1] K. S. Novoselov, A. K. Geim, S. V. Morozov, D. Jiang, Y. Zhang, V. Dubonos, I. V. Grigorieva, and A. A. Firsov, Science **306**, 666 (2004).
[2] K. S. Novoselov, D. Jiang, F. Schedin, T. J. Booth, V. V. Khotkevich, S. V. Morozov, and A. K. Geim, Proc. Natl. Acad. Sci. U.S.A. **102**, 10451 (2005).
[3] K. S. Novoselov, A. K. Geim, S. V. Morozov, D. Jiang, M. I. Katsnelson, I. V. Grigorieva, S. V. Dubonos, and A. A. Firsov, Nature (London) **438**, 197 (2005).
[4] Y. Zhang, J. Tan, H. L. Stormer, and P. Kim, Nature (London) **438**, 201 (2005).
[5] Y. Zhang, Z. Jiang, J. P. Small, M. S. Purewal, Y.-W. Tan, M. Fazlollahi, J. D. Chudow, J. A. Jaszczak, H. L. Stormer, and P. Kim, Phys. Rev. Lett. **96**, 136806 (2006).
[6] Z. Jiang, Y. Zhang, H. L. Stormer, and P. Kim, Phys. Rev. Lett. **99**, 106802 (2007).
[7] K. Nomura and A. H. MacDonald, Phys. Rev. Lett. **96**, 256602 (2006).
[8] J. Alicea and M. P. A. Fisher, Phys. Rev. B **74**, 075422 (2006).
[9] Kun Yang, S. Das Sarma, and A. H. MacDonald, Phys. Rev. B **74**, 075423 (2006).
[10] M. O. Goerbig, R. Moessner and B. Douçot, Phys. Rev. B **74**, 161407(R) (2006).
[11] M. Ezawa, J. Phys. Soc. Jpn. **76**, 094701 (2007).
[12] D. A. Abanin, P. A. Lee, and L. S. Levitov, Phys. Rev. Lett. **96**, 176803 (2006).
[13] D. V. Khveshchenko, Phys. Rev. Lett. **87**, 206401 (2001).
[14] V. P. Gusynin, V. A. Miransky, S. G. Sharapov, and I. A. Shovkovy, Phys. Rev. B **74**, 195429 (2006).
[15] E. V. Gorbar, V. P. Gusynin, and V. A. Miransky, Low Temp. Phys. **34**, 790 (2008).
[16] V. P. Gusynin, V. A. Miransky, S. G. Sharapov, and I. A. Shovkovy, Phys. Rev. B **77**, 205409 (2008).
[17] H. A. Fertig and L. Brey, Phys. Rev. Lett. **97**, 116805 (2006).
[18] Dmitry A. Abanin, Kostya S. Novoselov, Uli Zeitler, Patrick A. Lee, A. K. Geim, and L. S. Levitov, Phys. Rev. Lett. **98**, 196806 (2007).
[19] J. G. Checkelsky, L. Li, and N. P. Ong, Phys. Rev. Lett. **100**, 206801 (2008).

[20] K. Moon, H. Mori, Kun Yang, S. M. Girvin, A. H. MacDonald, L. Zheng, D. Yoshioka, and Shou-Cheng Zhang, Phys. Rev. B **51**, 5138 (1995).
[21] V. P. Gusynin, V. A. Miransky, and I. A. Shovkovy, Phys. Rev. Lett. **73**, 3499 (1994); Phys. Rev. D **52**, 4718 (1995).
[22] F. D. M. Haldane and D. N. Sheng (private communication).
[23] E. Shimshoni, H. A. Fertig, and G. Venketeswara Pai, arXiv:0807.2867 (unpublished).